Syntaxin 4 Expression in Pancreatic β-Cells Promotes Islet Function and Protects Functional β-Cell Mass

Eunjin Oh,[1] Miwon Ahn,[1] Solomon Afelik,[2] Thomas C. Becker,[3] Bart O. Roep,[4] and Debbie C. Thurmond[1]

Diabetes 2018;67:2626–2639 | https://doi.org/10.2337/db18-0259

Syntaxin 4 (Stx4) enrichment in human and mouse islet grafts improves the success of transplants in reversing streptozotocin (STZ)-induced diabetes in mice, although the underlying molecular mechanisms remain elusive. Toward a further understanding of this, human islets and inducible transgenic mice that selectively overexpress Stx4 in islet β-cells (βTG-Stx4) were challenged with proinflammatory stressors in vitro and in vivo. Remarkably, βTG-Stx4 mice resisted the loss of β-cell mass and the glucose intolerance that multiple low doses of STZ induce. Under standard conditions, glucose tolerance was enhanced and mice maintained normal fasting glycemia and insulinemia. Conversely, Stx4 heterozygous knockout mice succumbed rapidly to STZ-induced glucose intolerance compared with their wild-type littermates. Human islet β-cells overexpressing Stx4 exhibited enhanced insulin secretory capability; resilience against proinflammatory cytokine–induced apoptosis; and reduced expression of the *CXCL9*, *CXCL10*, and *CXCL11* genes coordinate with decreased activation/nuclear localization of nuclear factor-κB. Finding ways to boost Stx4 expression presents a novel potential therapeutic avenue for promoting islet function and preserving β-cell mass.

Type 1 diabetes (T1D) is linked to inflammation related to the damaging effects of proinflammatory cytokines on pancreatic islet β-cells (1,2). Data suggest that β-cell preservation and recovery interventions are most effective in individuals with the highest levels of residual β-cell function and insulin production (3). Even modest β-cell function upon entry into the Diabetes Control and Complications Trial (DCCT) correlated with reduced incidences of retinopathy, nephropathy, and hypoglycemic complications (4). As such, there is great interest in developing strategies to enhance the function of insulin secretion from residual β-cell mass in vivo and to protect islet β-cells from targeted demise.

Evidence suggests that β-cell dysfunction precedes and acts as an early predictor of T1D (5). One of the rate-limiting features of the insulin secretion process is the abundance of soluble n-ethylmaleimide-sensitive fusion protein-attachment protein receptor (SNARE) proteins in each β-cell. Insulin granules mobilized and juxtaposed to the cell surface undergo docking and fusion before β-cells release insulin; docking entails the pairing of protein complexes on the granule (vesicle SNAREs [VAMPs]) with their cognate receptor complexes at the target membrane (*t*-SNAREs) (6,7). Two types of *t*-SNAREs, syntaxins and SNAPs, and one v-SNARE combine to form a heterotrimeric SNARE core complex. Syntaxin 1A (Stx1A) and syntaxin 4 (Stx4) oversee glucose-stimulated insulin secretion (GSIS), pairing with VAMP2 or VAMP8 (8,9), along with SNAP25 (10). However, whereas Stx4 overexpression prompts improved glucose tolerance and GSIS in vivo (11,12), Stx1A enrichment results in β-cell failure, which is linked to Stx1A-specific regulation of ion channels (13).

Stx4 is a T1D candidate protein, predicted by in silico phenome-interactome network analysis (14); the *Stx4* gene is located within T1D susceptibility region Iddm10 (www.T1Dbase.org). In addition to Stx4, several other SNARE exocytosis proteins are notably deficient in T2D islets, yet remarkably, restoration of just Stx4 to those

[1]Department of Molecular and Cellular Endocrinology, Diabetes and Metabolism Research Institute of City of Hope, Duarte, CA
[2]Department of Surgery/Division of Transplantation, University of Illinois at Chicago, Chicago, IL
[3]Department of Internal Medicine, Duke Molecular Physiology Institute, Duke University, Durham, NC
[4]Department of Diabetes Immunology, Diabetes and Metabolism Research Institute of City of Hope, Duarte, CA

Corresponding author: Debbie C. Thurmond, dthurmond@coh.org.

Received 6 March 2018 and accepted 25 September 2018.

This article contains Supplementary Data online at http://diabetes.diabetesjournals.org/lookup/suppl/doi:10.2337/db18-0259/-/DC1.

E.O. and M.A. contributed equally to this work.

islets resulted in the resumption of biphasic GSIS (9). Given the established role of Stx4 in both phases of GSIS, this restored islet function was presumed to be related to the ability of Stx4 to overcome the need for the other missing exocytosis factors in the islets. Although promising, because of the limitations of previous studies it remains unclear whether Stx4 function in β-cell GSIS is the primary or sole mechanism underpinning the restored GSIS phenomenon; in those studies, the previously available Stx4 overexpression systems used in human islets and mice were not β-cell specific.

Hence, in this study we used β-cell-selective expression systems to demonstrate that Stx4 enrichment, in addition to its known beneficial role in β-cell function, correlates with ameliorating apoptosis, preserving β-cells from inflammation-induced destruction by tempering the nuclear factor (NF)-κB–induced CXCL9, CXCL10, and CXCL11 inflammatory program.

RESEARCH DESIGN AND METHODS

Mice

All mouse studies were conducted per the guidelines and assurances of the City of Hope Institutional Animal Care and Use Committee. Stx4 heterozygous (+/−) knockout mice were generated as previously described (12,15). To generate βTG-Stx4 mice, we bred commercially available rat insulin promoter (RIP)–reverse tetracycline-controlled transactivator (rtTA) mice (no. 008250; The Jackson Laboratory, Bar Harbor, ME), with our custom-generated TRE-Stx4 mice. The TRE-Stx4 mice were initially made through the use of B6 blastocyst injection (Indiana University School of Medicine Transgenic Core). Rat Stx4 cDNA was subcloned into the 5′ *Bam*HI and 3′ *Cla*I sites downstream of the tetracycline response element promoter; 29 founder mice were obtained, and four lines among these mice were phenotyped to show similar glucose and insulin tolerances. These mice were crossed with RIP-rtTA mice (RIP confers β-cell selectivity; tetracycline/doxycycline [Dox] induces binding of the TRE to elicit expression of the transgene). Mouse insulin promoter (MIP)–rtTA mice were a gift from Philip Scherer (University of Texas Southwestern Medical Center), and we used them, where indicated, in place of the RIP-rtTA, as previously described (16,17). βTG-Stx4 transgenic mice were provided drinking water containing Dox (1–2 mg/mL acidified water kept in dark red bottles to protect it from light) or regular drinking water for at least 3 weeks before experiments to yield stabilized transgene expression.

Antibodies and Cytokines

Stx4 antibody was generated for use in immunoblotting mouse islets, as previously described (18,19). Stx4 for human islets (Chemicon International, Temecula, CA); tubulin (Sigma-Aldrich, St. Louis, MO); cleaved caspase-3 (CC-3), total NF-κB (t-NF-κB), phosphorylated NF-κB (p-NF-κB), and TATA binding protein (Cell Signaling Technology, Beverly, MA); and goat antirabbit–horseradish peroxidase and antimouse–horseradish peroxidase secondary antibodies (Bio-Rad, Hercules, CA) were used for immunoblotting. Enhanced chemiluminescence and ECL Prime reagents were purchased from Thermo Fisher Scientific. For immunohistochemistry, antibodies against Stx4 were purchased from Chemicon International; against glucagon, from Abcam; and against insulin, from Dako. Proinflammatory cytokines were purchased from ProSpec-Tany Technogene Ltd (East Brunswick, NJ) as described elsewhere (20).

Intraperitoneal Glucose Tolerance Test and Insulin Tolerance Test

Blood samples were collected after male and female knockout or transgenic mice were deprived of food, then freshly made D-glucose was injected intraperitoneally into the mice for intraperitoneal glucose tolerance tests (IPGTTs). For the insulin tolerance test, the same mice were deprived of food for 6 h (0800–1400 h), and after blood was collected, the mice were injected intraperitoneally with Humulin R (0.75 unit/kg body wt) (Eli Lilly & Co., Indianapolis, IN).

Multiple Low-Dose Streptozotocin Protocol

Male mice were subjected to an IPGTT at 10 weeks of age, before the multiple low-dose streptozotocin (MLD-STZ) protocol was initiated (21). Mice were injected with STZ (35 mg/kg body wt) for 5 consecutive days. Five days later (10 days after the first injection), $Stx4^{+/+}$ (wild-type) and $Stx4^{+/-}$ mice were deprived of food for 6 h (0800 h–1400 h), blood samples were collected to measure blood glucose, and then the mice were injected intraperitoneally with glucose (1 g/kg body wt) and the blood sampled from the tail vein every 30 min through the use of a glucometer (HemoCue, Mission Viejo, CA), to again measure blood glucose. Male βTG-Stx4 mice were given Dox (2 mg/mL) in drinking water for 3 weeks before the MLD-STZ injections were begun. A total of 24 days after initiating the MLD-STZ protocol, βTG-Stx4 or non-Dox-treated (control) mice were deprived of food for 6 h (0800 h–1400 h), then injected intraperitoneally with glucose (2 g/kg body wt), after which we performed the IPGTTs.

Isolation, Immunoblotting, and Secretion Assays With the Use of Transgenic Mouse Islets

Pancreatic mouse islets were isolated, as previously described (22), from 10- to 14-week-old male and female mice, as noted in the figure legends. Islets cultured overnight were manually placed in microcentrifuge tubes containing Krebs-Ringer bicarbonate buffer (10 mmol/L HEPES [pH 7.4], 134 mmol/L NaCl, 5 mmol/L $NaHCO_3$, 4.8 mmol/L KCl, 1 mmol/L $CaCl_2$, 1.2 mmol/L $MgSO_4$, 1.2 mmol/L KH_2PO_4) containing 2.8 mmol/L glucose and 0.1% BSA and left for 1 h. Then the buffer was changed to either 16.7 mmol/L or 2.8 mmol/L and left for another hour to contain with 16.7 mmol/L glucose or 2.8 mmol/L glucose. The supernatant was collected for use in quantitating insulin release by radioimmunoassay (Millipore).

Islets were subsequently harvested in 1% NP-40 lysis buffer (1% NP-40, 25 mmol/L HEPES [pH 7.4], 10% glycerol, 50 μmol/L sodium fluoride, 10 mmol/L sodium pyrophosphate, 1 mmol/L sodium vanadate, 137 mmol/L sodium chloride, 1 mmol/L phenylmethylsulfonyl fluoride, 1 μg/mL pepstatin, and 10 μg/mL aprotinin) for use in evaluating total protein or insulin content, as previously described (23).

TUNEL Staining and Morphometric Assessment of Islet Cell Mass

Pancreatic sections were immunostained with guinea pig anti-insulin (1:200 dilution) (DAKO). We used the Alexa Fluor 488 goat anti–guinea pig secondary antibody (1:500 dilution) (Invitrogen) to detect insulin-positive β-cells. We used the TUNEL In Situ TMR Red Cell Death Detection Kit (Roche, Mannheim, Germany) to stain apoptotic cells. Sections were scanned with the use of a microscope (Keyence fluorescence miroscope; Keyence, Itasca, IL). Results were expressed as the percentage of cells with positive TUNEL staining relative to the total number of insulin-positive cells. Mouse islet morphometry was evaluated using anti-insulin immunohistochemical staining of pancreatic sections, as described previously (23).

Human Islet Transduction, RNA Isolation, RNA Sequencing, and Quantitative Real-time PCR

Human islets were obtained from the Integrated Islet Distribution Program or the City of Hope Islet Core (donor information can be found in Supplementary Table 1). Upon receipt, human islets were first allowed to recover in Connaught Medical Research Laboratories medium for 2 h; then they were manually placed under a light microscope, which was equipped with a green gelatin filter to discriminate residual nonislet material. For generating adenovirus, rat Stx4 cDNA was subcloned into the 5′ *Eco*RI and 3′ *Bam*HI sites of the FN611 adenoviral vector that contains the Ins1 promoter/RIP (24). Adenoviruses were packaged with green fluorescent protein (Rous sarcoma virus promoter [RSV-GFP] in the E3 region) to visually identify transduced cells (Viraquest, North Liberty, IA). Human islets were transduced with Ad-RIP-Stx4 or Ad-RIP-Ctrl adenovirus (multiplicity of infection [MOI], 100) for 1 h, washed with PBS, and incubated with CMRL-1066 medium for 48 h; we used these islets for perifusion analysis (22) or to isolate RNA (RNeasy Plus Mini Kit [QIAGEN] processed with a TruSeq Stranded mRNA Library Prep Kit [Illumina]). The RNA integrity numbers for all samples were ≥8.0. We aligned reads against hg19 using TopHat2. Read counts were tabulated using htseq-count, with University of California Santa Cruz known gene annotations (TxDb.Hsapiens.UCSC.hg19.knownGene annotation package in R software). Fold change values were calculated from reads per kilobase per million reads and normalized expression values, which we also used for visualization (after a log2 transformation). We calculated *P* values from raw counts with the use of edgeR, and false discovery rates were calculated. Before calculating *P* values, we filtered genes to include only transcripts with a reads per kilobase per million reads expression level of 0.1 in at least 50% of samples and genes that were longer than 150 base pairs. Genes were defined as differentially expressed if they had a fold change >1.5 and a false discovery rate <0.05. Gene ontology enrichment was calculated through the use of goseq. Additional systems-level analysis was performed in the Ingenuity Pathway Analysis tool (www.ingenuity.com; Ingenuity Systems). RNA sequencing data were confirmed by quantitative RT-PCR (Supplementary Table 2).

EndoC-βH^1, MIN6, and INS-1 832/13 Cell Cultures

EndoC-βH^1 cells obtained from Dr. Roland Stein (Vanderbilt University) were cultured as described previously (25). MIN6 and INS-1 832/13 cells (also cultured as previously described [20,26]) were adenovirally transduced (MOI, 50–100) for 2 h, washed with PBS, and incubated for 48 h. Cells were treated for the last 16 h (EndoC-βH^1 and INS-1 832/13) or 24 h (MIN6) in medium containing proinflammatory cytokines (19) and cleared detergent cell lysates prepared for immunoblotting, or RNA was isolated for quantitative real-time PCR (Supplementary Table 2).

Adenoviral shRNA-Mediated Knockdown of Stx4

The shRNA sequences for mouse Stx4 adapted from the plasmid-based pSilencer1.0-Stx4 (26) were subcloned into the 5′ *Afl*II and 3′ *Spe*I sites of the pSilencer-Adeno-CMV vector (Thermo Fisher Scientific), and the adenovirus was purified with CsCl at Viraquest Inc.(North Liberty, IA). MIN6 cells were transduced at an MOI of 50–100 for 2 h, washed with PBS, then incubated for 24 h in MIN6 complete medium and for another 24 h in medium containing proinflammatory cytokines (19). RNA was isolated for use in quantitative real-time PCR (Supplementary Table 2).

Subcellular Fractionation of Human Islet and INS-1 832/13 Cells

Transduced human islets or INS-1 832/13 cells either were treated with proinflammatory cytokines (10 ng/mL tumor necrosis factor [TNF]-α, 100 ng/mL interferon [IFN]-γ, and 5 ng/mL interleukin [IL]-1β) for 16 h then harvested as detergent cell lysates, or were partitioned into nuclear and nonnuclear fractions through the use of an NE-PER Nuclear and Cytoplasmic Extraction Kit (Thermo Fisher Scientific). We used the fractions for immunoblot analyses to localize t-NF-κB and p-NF-κB.

Immunofluorescent Confocal Imaging

Pancreata from βStx4-dTg mice that were treated with Dox or that did not receive Dox were fixed in 4% paraformaldehyde and embedded in paraffin. Slides were dewaxed, rehydrated, and stained with guinea pig anti-insulin (1:500), mouse pig antiglucagon (1:200), and rabbit anti-Stx4 (1:100) antibodies at 4°C overnight. Stained pancreata were washed and incubated with Alexa Fluor 488–, 647–, or 568–conjugated secondary antibodies (1:500), respectively, for 1 h. The pancreata were washed again and

overlaid with Vectashield mounting medium. INS-1 832/3 cells were transduced with Ad-RIP-Stx4 or the control adenovirus for 1 h, washed with PBS, and incubated in complete medium for 48 h; proinflammatory cytokines were added for the last 16 h. The cells were fixed in 4% paraformaldehyde and stained with rabbit anti-CC-3 (1:100) and mouse NF-κB (1:100) antibodies at 4°C overnight. The cells were washed and incubated with Alexa Fluor 568– or 647–conjugated secondary antibodies (1:500), respectively, for 1 h and then washed. We used DAPI stain to detect nuclei. Cells were subsequently overlaid with Vectashield mounting medium for imaging with a Zeiss 700 confocal microscope with a 40× objective (6× zoom was applied to magnify the images).

Quantification and Statistical Analysis

All data were evaluated for statistical significance through the use of the Student *t* test for pairwise comparison of two groups (i.e., $Stx4^{+/-}$ vs. $Stx4^{+/+}$), or with ANOVA with the Tukey post hoc test in GraphPad Prism software. Data are expressed as the mean ± SEM and are considered statistically significant when $P < 0.05$. Box-and-whisker plots denote the minimal to maximal values.

RESULTS

Selective Overexpression of Stx4 in β-Cells Is Sufficient to Boost Glucose Tolerance

To study the impact of Stx4 upregulation selectively in the β-cells of adult mice, we designed a Dox-inducible double transgenic model: Dox-induced expression of the RIP-rtTA or MIP-rtTA transgene drives TRE-Stx4 transgene expression, conferring β-cell-selective expression of Stx4 (Fig. 1*A*). This design allays any concerns over developmental changes that may occur with transgene expression. In this model, Stx4 expression is increased approximately two- to threefold over endogenous levels in islets of double transgenic (βTG-Stx4) mice in response to Dox (Fig. 1*B*). Per the design of the model, the βTG-Stx4 mice did not overexpress the Stx4 transgene in the hypothalamus, showing levels similar to those in control mice (non-Dox-treated double transgenic line or the RIP-rtTA single transgenic line) (Fig. 1*B*); nor was the transgene overexpressed in the islet α-cells (Fig. 1*C*). Stx4 was principally localized in the plasma membrane, as indicated by intracellular labeling, as previously demonstrated and expected for this plasma membrane *t*-SNARE protein in β-cells (12). Stx4 abundance did not change in tissues such as heart, lung, liver, kidney, spleen, skeletal muscle, and epigonadal fat, nor did the levels of its binding partners change (Supplementary Fig. 1*A*). Dox-treated female βTG-Stx4 mice exhibited enhanced glucose tolerance in IPGTT assays than did the control (non-Dox-treated double transgenic) mice (Fig. 1*D*) and the single transgenic mice treated with or not treated with Dox (Supplementary Fig. 1*B*). Dox-treated βTG-Stx4 mice showed no change in insulin tolerance when compared with non-Dox-treated controls (Fig. 1*E*). This pattern of transgene expression and physiological response was fully recapitulated in a second founder line (Supplementary Fig. 2*A–C*). MIP-rtTA-based βTG-Stx4 mice served as a second model to study β-cell-specific Stx4 overexpression in vivo; MIP-based female βTG-Stx4 mice phenocopied the RIP-based βTG-Stx4 mice (Supplementary Fig. 3*A–C*). These data indicate that the upregulation of Stx4 strictly in β-cells can promote enhanced glucose tolerance.

Serum insulin content was measured during the IPGTT to assess the magnitude of the in vivo acute response to the glucose stimulus. Dox-treated βTG-Stx4 mice elicited a significant acute increase in serum insulin content within 10 min of glucose injection compared with non-Dox-treated mice (Fig. 1*F*). It is important to note that basal insulin release in the Dox-treated βTG-Stx4 mice was similar to that in control mice, indicating that the "boosting" effect of Stx4 on function allows the mice to retain normal responsiveness to glucose and does not cause aberrant elevation of insulin release under basal conditions. Islets isolated from our βTG-Stx4 mice show more than twofold potentiation of GSIS in static islet culture assays (Fig. 1*G*). This level of enhancement is notably proportional to the approximately two- to threefold increased abundance of Stx4 protein in the islets. No differences were found in serum triglycerides, cholesterol, nonesterified fatty acids, or glucagon levels between the control and the βTG-Stx4 mice that were deprived of food for either 16 h or 6 h (Supplementary Table 3); similarly, no differences were detected in body weights or organ and tissue weights (Supplementary Table 4). Taken together, the results of our studies indicate that the effect of Stx4 on β-cells accounts for its positive effect on islet function. These data also indicate an increased secretory capacity in the mice that selectively overexpress Stx4 in β-cells.

Mice Overexpressing β-Cell-Specific Stx4 Resist STZ-Induced Diabetes

To test the working hypothesis that Stx4 abundance is crucial to the defense against diabetes induced by proinflammatory cytokines, young male Stx4 heterozygous ($Stx4^{+/-}$) knockout mice were subjected to MLD-STZ treatment (male C57Bl6J mice are more sensitive to STZ [27]). While male $Stx4^{+/-}$ mice exhibited glucose intolerance at older ages (15), younger mice were not yet impaired, as determined by IPGTT (2 g glucose/kg body wt) (Fig. 2*A*). However, young $Stx4^{+/-}$ mice treated with MLD-STZ were more severely glucose intolerant that wild-type control littermates within 10 days of initiating the protocol (using 1 g glucose/kg body wt), concurrent with significantly elevated levels of TUNEL-positive β-cells (Fig. 2*B* and *C*). These data suggest that a partial depletion of Stx4 may correlate with an increased susceptibility to inflammatory damage to β-cells in vivo.

To determine whether the selective increase of Stx4 in the β-cells of the mice could offer protection against inflammatory damage associated with diabetes, Dox-treated male βTG-Stx4 mice were challenged with MLD-STZ in

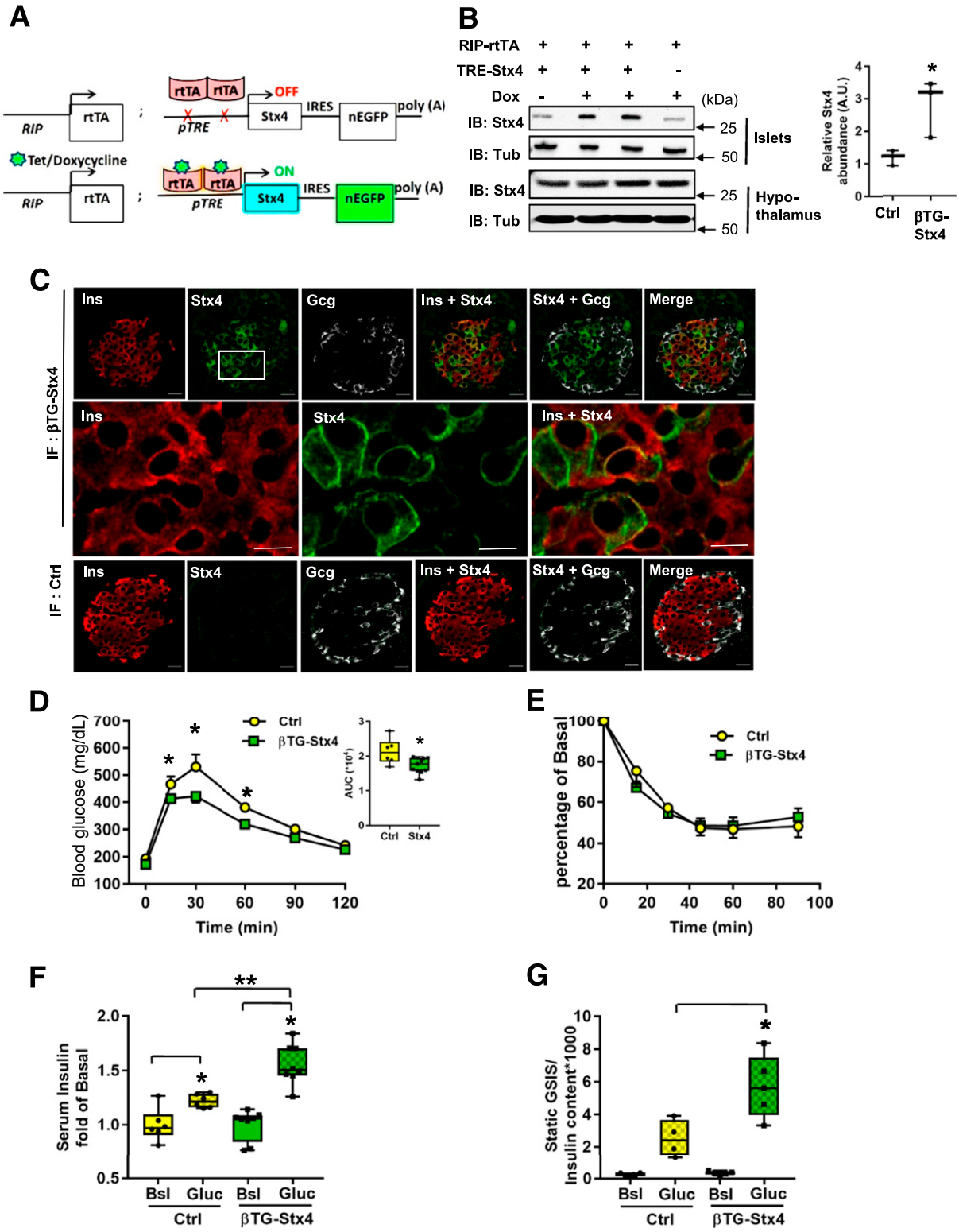

Figure 1—Selective Stx4 enrichment in mouse islet β-cells improves glucose tolerance and islet function in response to glucose. *A*: Design strategy of the βTG-Stx4 mouse model. RIP- or MIP-rtTA$^{+/-}$ transgenic mice were crossed with TRE-Stx4$^{+/-}$ transgenic mice to generate Dox-inducible β-cell-specific Stx4 overexpression in islet β-cells in adult βTG-Stx4 mice. *B*: RIP-based βTG-Stx4 mice show Dox-inducible Stx4 overexpression in islets but not in the hypothalamus (left). The bar graph to the right quantitates values from three mice per group. *$P <$ 0.05, control (Ctrl) (−Dox-βTG-Stx4) vs. βTG-Stx4 (+Dox-βTG-Stx4). *C*: β-Cell-specific Stx4 overexpression was confirmed in isolated mouse islet β-cells through the use of immunofluorescent confocal microscopy colocalization of insulin (Ins). We observed no colocalization in glucagon (Gcg)-stained α-cells (n = 3–5 islets from each of three βTG-Stx4 mice). Scale bars = 20 μm. Middle row: original magnification ×6 of the boxed portion of the second image in the top panels. Scale bars = 10 μm. *D* and *E*: IPGTT (*D*) and intraperitoneal insulin tolerance tests (*E*) of Ctrl (yellow) and Dox-treated female βTG-Stx4 mice (green). The inset graph in *D* shows area under the curve (AUC) analyses of IPGTT

parallel with non-Dox-treated double transgenic mice (control) and assessed by IPGTT (2 g glucose/kg body wt both before and after STZ). Before STZ treatment, Dox-treated male βTG-Stx4 mice were more glucose tolerant than control mice (Fig. 2*D*). At 24 days after initiating the MLD-STZ protocol, control mice exhibited severe glucose intolerance, whereas Dox-treated βTG-Stx4 mice retained more normal levels of glucose tolerance and fasting blood glucose (Fig. 2*E* and *F*). Pancreata from Dox-treated βTG-Stx4 mice receiving MLD-STZ show fewer TUNEL-positive β-cells than MLD-STZ-treated control mice, as well as a preserved β-cell mass (Fig. 2*G* and *H*). MIP-based βTG-Stx4 mice also were protected against the MLD-STZ-induced severe fasting hyperglycemia (>400 mg/dL) and glucose intolerance observed in the paired control mice (Supplementary Fig. 3*D–F*). These data indicate that Stx4 enrichment in β-cells, provided to adult mice rather than during development, was sufficient to confer protection against diabetogenic stimuli targeting islet β-cells.

RNA Sequencing of Human Islets That Specifically Overexpress Stx4 in β-Cells

To determine the potential contributing factors underlying the protection of Stx4-overexpressing β-cells against inflammatory damage, we used an adenovirus to drive Stx4 expression and the RIP promoter to drive an approximately two- to threefold increase in Stx4 expression selectively in β-cells of human islets (Fig. 3*A*); rat Stx4 colocalized with insulin-stained β-cells and was not observed in glucagon-stained α-cells (Fig. 3*A*). Human islets harboring the extra Stx4 showed increased function in each phase of GSIS (Fig. 3*B* and *C* and Supplementary Fig. 4). These data mimicked previously observed effects, which were obtained through the use of a cytomegalovirus-based Stx4 adenoviral expression system (9), validating the actions of Stx4 in the β-cells as being largely accountable for the improved function observed in the previous study. Human islets were subsequently transduced with Ad-RIP-Stx4 and were compared with Ad-RIP-Ctrl-transduced islets for differential gene expression; we used RNA sequencing as a means to identify mechanisms underlying the Stx4-mediated benefits to β-cells. The RNAseq output results in each of three independent sets of donor islets transduced with Ad-RIP-Ctrl or Ad-RIP-Stx4 showed clear clustering by virus type alone (Fig. 3*D*). Differential gene expression analyses pointed to endocrine systems, metabolism, and immunological diseases (Supplementary Table 5). Canonical pathways identified by Ingenuity Pathway Analysis included mainly immune pathways, showing that the downregulation of genes such as *CXCL9*, *CXCL10*, and *CXCL11*, which are implicated in apoptosis and islet inflammation, coordinates with the increased Stx4 (Supplementary Table 5). Quantitative RT-PCR confirmed the RNA sequencing results (Fig. 3*E*). The infection process itself induced the increased expression of these chemokines (Supplementary Table 6), as has been reported previously (28); Ad-RIP-Stx4 cells showed significantly less expression of these chemokine ligands than that in Ad-RIP-Ctrl cells in every independent batch of human donor islets tested.

Stx4 Levels Are Inversely Proportional to Proinflammatory Cytokine–Induced Expression of CXCL9 and CXCL10 in β-Cells

Proinflammatory cytokines are used to mimic the diabetogenic milieu by promoting loss of β-cell mass (29) and increasing the expression of CXCL9, CXCL10, and CXCL11 (30). Transduced INS-1 832/13 cells were exposed to a cocktail of tumor necrosis factor-α, interleukin-1β, and interferon-γ for 16 h, and the levels of the chemokine ligands were evaluated by quantitative RT-PCR. Chemokine levels were elevated by treating β-cells with proinflammatory cytokines, as otherwise levels remain very low (31), even with adenoviral transduction (28). In INS-1 832/13 cells transduced with Ad-RIP-Ctrl and treated with cytokines, significant fold elevations in CXCL9, CXCL10, and CXCL11 expression were observed. After setting these fold increases at 100%, we discovered that INS-1 cells transduced with Ad-RIP-Stx4 showed substantial reductions of cytokine-induced CXCL9 and CXCL10 expression by comparison (Fig. 4*A* and Supplementary Fig. 5*A*). This finding was also seen in the mouse MIN6 β-cell line, in which cytokine-induced CXCL11 expression was also significantly reduced in Stx4-overexpressing cells (Fig. 4*B* and Supplementary Fig. 5*B*). We next questioned whether Stx4 depletion could exert the opposite effect on CXCL9 expression. We depleted MIN6 β-cells of Stx4 using Ad-shRNA, and in these cells CXCL9 expression increased ~18-fold under cytokine-treated conditions, a significant increase over that induced by Ad-Ctrl shRNA and cytokines (Fig. 4*C*, right, bar 4 vs. bar 2). Notably, Stx4 depletion alone, without exposure to cytokines, evoked a significant increase in CXCL9 expression (Fig. 4*C*, right, bar 3 vs. bar 1). This finding supports the concept that Stx4 deficiency correlates with an increased susceptibility to β-cell stress, as was seen in the STZ-treated $Stx4^{+/-}$ mice (Fig. 2*B* and *C*).

β-Cell Stx4 Expression Correlates With Reduced Proinflammatory Cytokine–Induced NF-κB Translocation and Apoptosis

We used network analysis to model potential linkages among the hits in our differential expression data set,

(*n* = 6–11 mice; **P* < 0.05). *F*: Serum insulin content in female Ctrl or Dox-treated βTG-Stx4 mice (*n* = 6–8 per group) that were deprived of food for 6 h (basal conditions [Bsl]) or stimulated with glucose for 10 min (Gluc). **P* < 0.05 vs. Bsl; ***P* < 0.05, glucose-stimulated Ctrl vs. βTG-Stx4. *G*: Ex vivo static GSIS/insulin content from islets isolated from female Ctrl and Dox-treated βTG-Stx4 mice (*n* = 4 or 5 sets of islets per group). **P* < 0.05, glucose-stimulated Ctrl vs. βTG-Stx4. IB, immunoblot; IF, immunofluorescence; IRES, internal ribosome entry site; nEGFP, nuclear enhanced green fluorescence protein; Tet, tetracycline; Tub, tubulin.

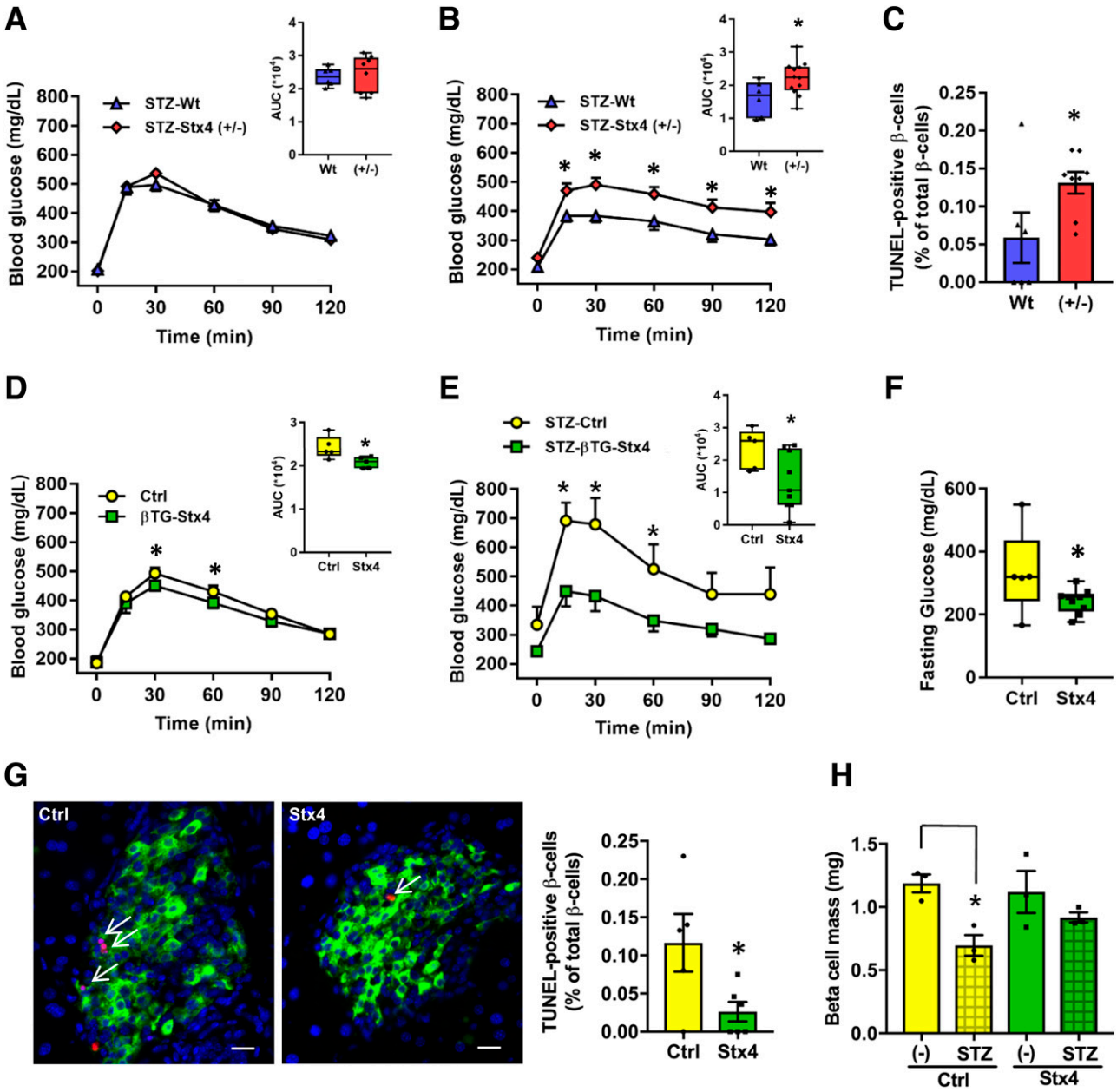

Figure 2—Stx4 abundance positively correlates with improved glucose tolerance and functional β-cell mass. *A*: Partial Stx4 deficiency heightens susceptibility to MLD-STZ-induced dysregulation of glucose homeostasis. Young male Stx4 heterozygous knockout mice ($Stx4^{+/-}$) and wild-type (wild-type littermate mice were tested with an IPGTT (2 g glucose/kg body wt) before STZ treatment) (n = 6–8 mice per genotype; $P > 0.05$, not significant). *B*: Male mice were subjected to an MLD-STZ protocol (treatment with 35 mg STZ/kg body wt for 5 consecutive days). Ten days after initiating the MLD-STZ protocol, mice were subjected to an IPGTT (1 g glucose/kg body wt; n = 6–8 male mice per genotype). *C*: TUNEL immunofluorescent staining and quantification of TUNEL-positive β-cells (as a percentage of total β-cells) from pancreata of the MLD-STZ-treated wild-type or $Stx4^{+/-}$ mice (n = 6–8 mice per genotype). *D*: Dox-treated (βTG-Stx4) or nontreated (control [Ctrl]) male mice were tested with an IPGTT (2 g glucose/kg body wt) before STZ treatment (n = 7 or 8 mice per group). *E*: Mice were reassessed by IPGTT 24 days after the MLD-STZ protocol was initiated. *F*: Blood glucose levels were measured in MLD-STZ-treated Ctrl or βTG-Stx4 male mice after they had been deprived of food for 6 h (n = 5 mice for each genotype). *G*: TUNEL immunofluorescent staining (left) and quantification of TUNEL-positive β-cells (as a percentage of total β-cells; right) from pancreata of MLD-STZ-treated Ctrl or βTG-Stx4 mice (n = 5 or 6 pancreata per group). Scale bars = 20 μm. Arrows denote representative TUNEL-positive cells. *H*: Islet β-cell mass is preserved in MLD-STZ-treated Dox-treated male βTG-Stx4 mice (n = 3 or 4 pancreata per group). *$P < 0.05$. The inset graphs in *A*, *B*, *D*, and *E* show the area under the curve (AUC). Wt, wild type.

revealing a potential association between Stx4 and NF-κB (Fig. 5*A*). Indeed, phosphorylated NF-κB is known to translocate to the nuclei and transactivate promoters of CXCL9 and CXCL10 in stressed islet β-cells (32,33). To test this as a potential mechanism, human islets transduced with Ad-RIP-Ctrl or Ad-RIP-Stx4 were subfractionated to partition nuclear from nonnuclear proteins, and the locale of t-NF-κB and p-NF-κB determined by immunoblotting.

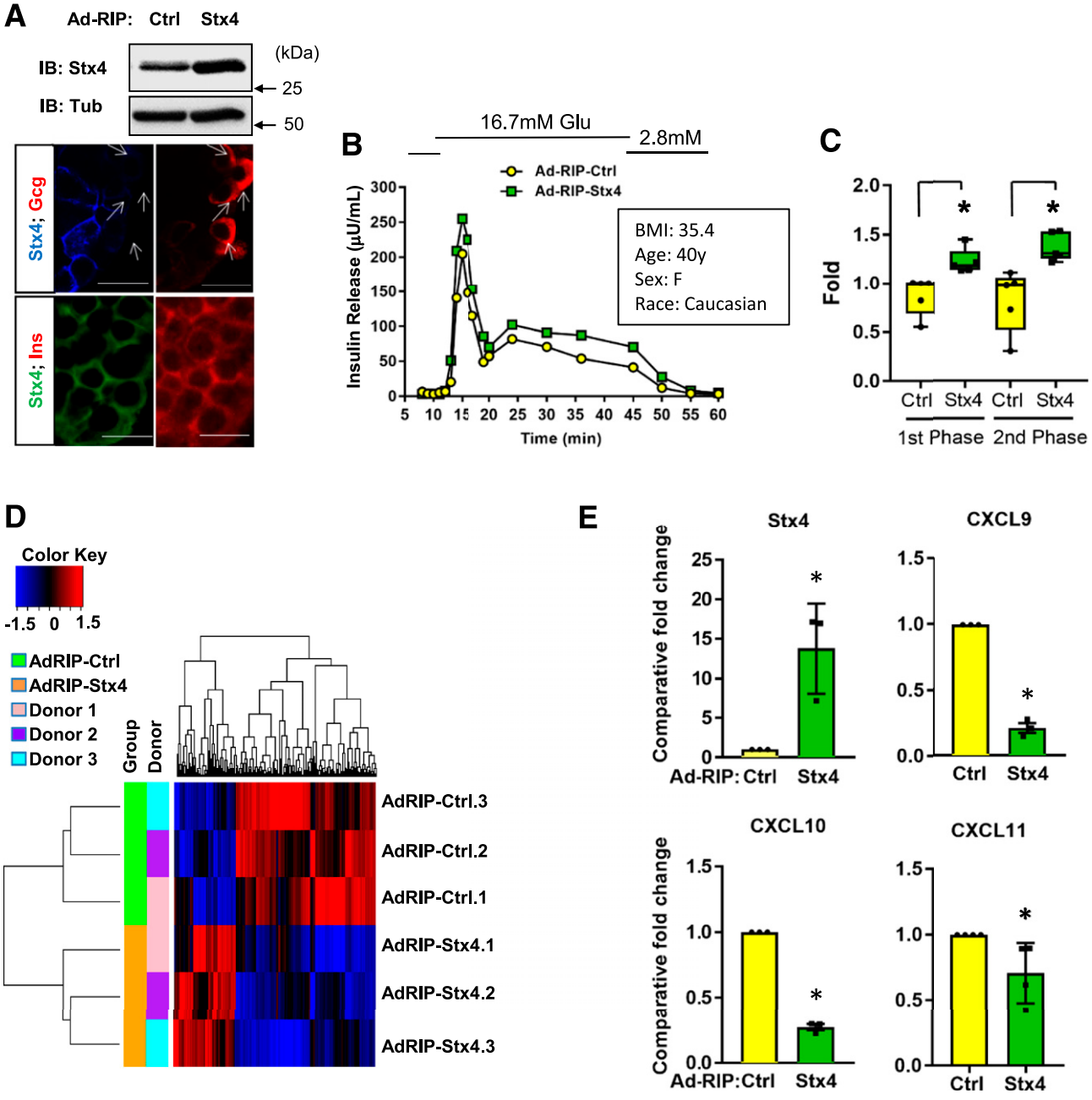

Figure 3—Selective overexpression of Stx4 in human islet β-cells improves function and ameliorates the infection-induced elevation of chemokine ligands CXCL9, CXCL10, and CXCL11. *A*: Human islets transduced to express Stx4 (Ad-RIP-Stx4) in order to selectively enrich Stx4 in β-cells of the islets, to colocalize with insulin (Ins), and to not be overexpressed glucagon (Gcg)-stained α-cells. Arrows denote the location of α-cells, superimposed on Stx4-stained images captured by dual-laser scanning confocal immunofluorescent microscopy. Scale bars = 20 μm. Ctrl, control. *B*: Ad-RIP-Stx4 overexpression in human islets promotes the amplitude of each phase of insulin release in perifusion analyses. A representative trace of five independent sets of human donor islets is shown (see Supplementary Fig. 4 for other traces). *C*: Calculated stimulation index response (stimulation index = glucose-stimulated secretion ÷ basal insulin secretion) of the area under the curve for each phase of insulin release (first phase = minutes 11–18; second phase = minutes 19–45, as described previously [9]); $n = 5$ donor islet sets per group). $^*P < 0.05$, Ad-RIP-Ctrl vs. Ad-RIP-Stx4. *D*: RNA sequencing of three independent batches of human donor islets transduced with either Ad-RIP-Stx4 or Ad-RIP-Ctrl. The heat map shows the clustering of differentially expressed genes grouped by virus type. *E*: Quantitative real-time PCR was performed to confirm Stx4 overexpression and three major hits: expression of CXCL9, CXCL10, and CXCL11. Values for Ad-RIP-Ctrl were set equal to 1.0 in each of the four sample sets, and the remaining groups were normalized to that value. Bars represent the mean ± SE ($n = 4$). $^*P < 0.05$. IB, immunoblot; Tub, tubulin.

Fig. 5*B* shows an ~40% decrease of t-NF-κB in nuclear fractions made from Stx4-overexpressing human islets. This does not occur through a direct association of Stx4 with NF-κB in β-cells (Supplementary Fig. 5). In addition, we evaluated the compound effect of proinflammatory cytokines to evoke NF-κB translocation into nuclear fractions from Ad-RIP-Ctrl in fractions from Ad-RIP-Ctrl and Ad-RIP-Stx4-overexpressing INS-1 832/13 β-cells.

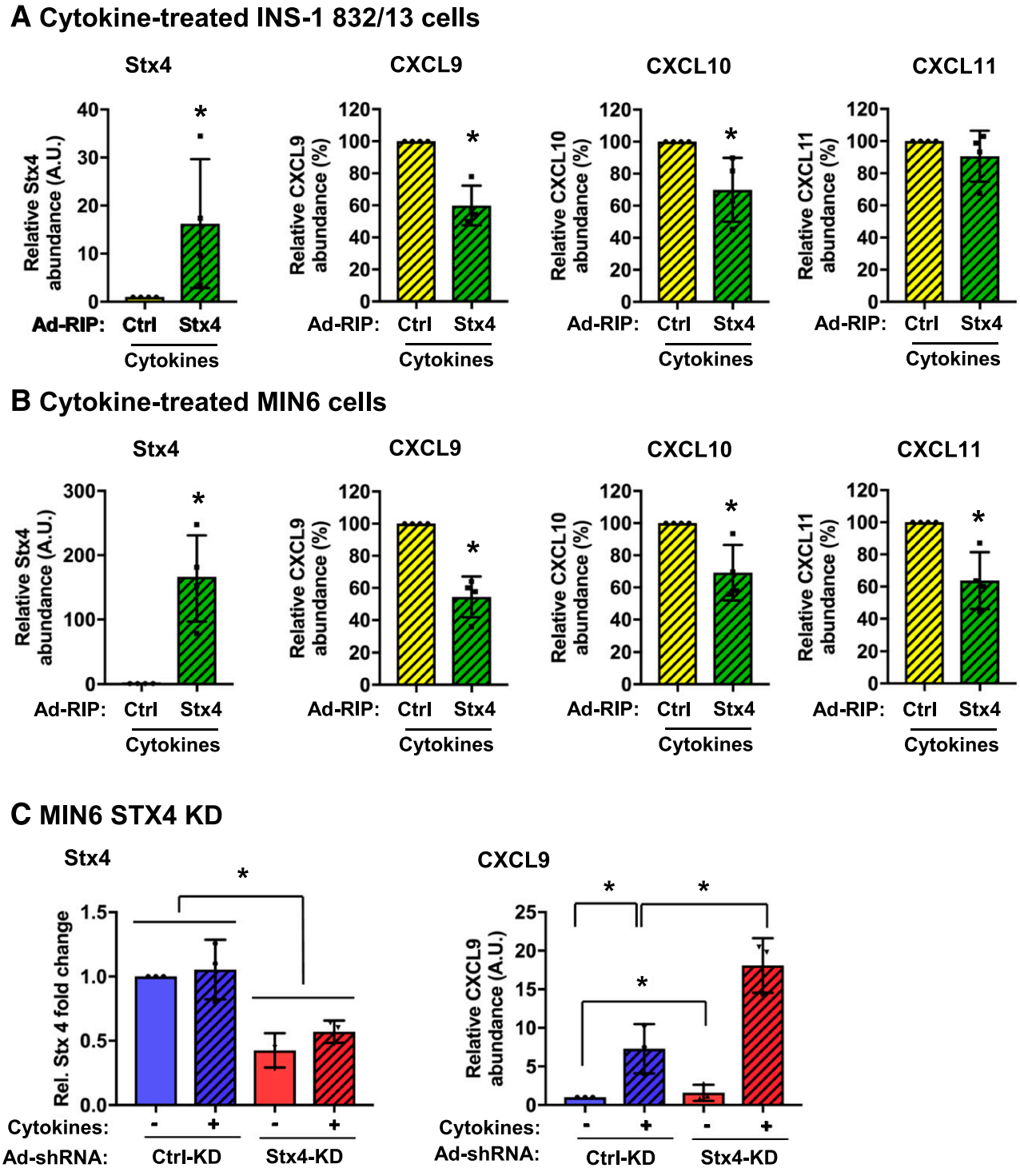

Figure 4—Stx4 enrichment reduces the cytokine-induced elevation of chemokine ligands in β-cells. *A*: INS-1 832/13 β-cells transduced with either Ad-RIP-Stx4 or Ad-RIP-Ctrl were exposed to a proinflammatory cytokine cocktail (TNF-α, IL-1β, IFN-γ; see RESEARCH DESIGN AND METHODS) for 16 h. Then the RNA was extracted for quantitative RT-PCR analysis of Stx4, CXCL9, CXCL10, and CXCL11. Fold increases due to cytokine stimulation were tabulated; the Ad-Ctrl was set equal to 100% in each of the four sample sets, and the remaining groups were normalized to that value. Bars represent the mean ± SE ($n = 4$). *B*: Similar analyses were performed with MIN6 β-cells treated with the cytokine cocktail for 24 h. *C*: Stx4 depletion from MIN6 β-cells. MIN6 cells were transduced with Ad-shRNA targeting mouse Stx4 (Stx4-KD) or control shRNA (Ctrl-KD); 24 h later they were exposed to the cytokine cocktail for another 24 h. RNA was extracted and evaluated by using quantitative RT-PCR to determine Stx4 and CXCL9 levels ($n = 3$ independent cell passages). *$P < 0.05$. A.U., arbitrary units.

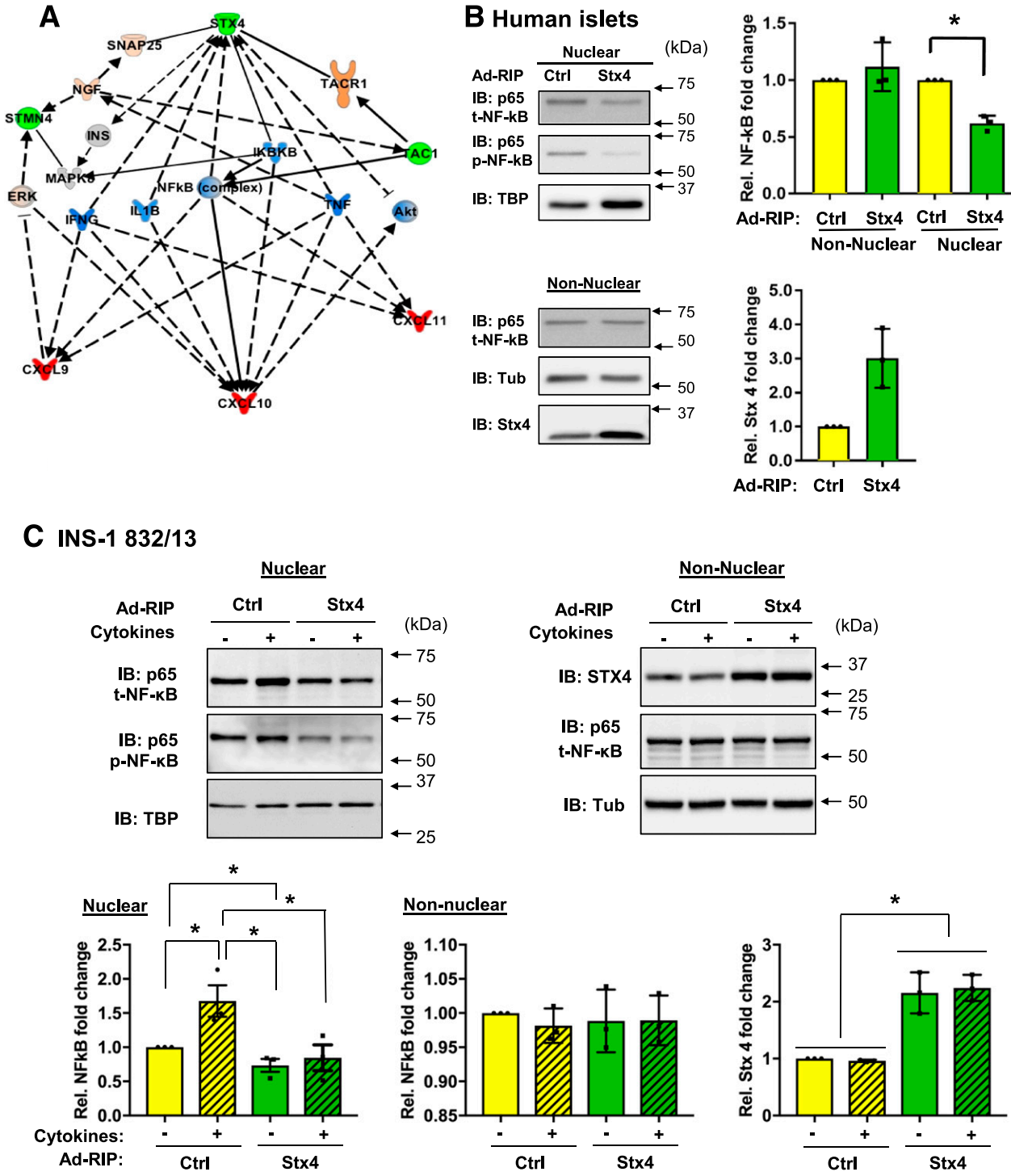

Figure 5—Stx4 enrichment correlates with attenuated nuclear NF-κB localization. *A*: RNA sequencing data from human islets transduced with Ad-RIP-Stx4 or Ad-RIP-Ctrl (as described in Fig. 3) were used to generate an Ingenuity Pathway Analysis network. *B*: Human islets transduced as described in Fig. 3 were harvested for subcellular fractionation into nuclear and nonnuclear fractions, and the localization of t-NF-κB and p-NF-κB proteins therein was assessed through the use of immunoblotting. Nonnuclear Stx4 or t-NF-κB was normalized to tubulin, and nuclear t-NF-κB was normalized to TATA binding protein. Stx4 was found only in the nonnuclear fraction, as expected; elevated Stx4 expression validated the virus transduction. Data represent the means of values from three independent batches of human donor islets. *$P < 0.05$ the Ad-RIP-Ctrl vs. the Ad-RIP-Stx4 nuclear fraction of t-NF-κB. *C*: INS-1 832/13 β-cells were transduced with Ad-RIP-Stx4 or Ad-RIP-Ctrl, and after 32 h of incubation cytokines were added for an additional 16 h. Cells were harvested for subcellular fractionation as described for panel *B*. Data represent the means of values from three independent passages of INS-1 832/13 cells. *$P < 0.05$. CXCL, chemokine (C-X-C motif) ligand; ERK, extracellular signal–regulated kinase; IB, immunoblot; IFNG, interferon γ; IKBKB, inhibitor of NF-κB kinase subunit β; IL1B; interleukin 1β; MAPK8, mitogen-activated protein kinase 8; NGF, nerve growth factor; Rel., relative; SNAP25, synaptosomal-associated protein 25; STMN4, stathmin 4; STX4, syntaxin 4; TAC1, tachykinin, precursor 1; TACR1, tachykinin receptor 1.

Stx4-expressing cells showed ablated cytokine-induced NF-κB translocation into the nuclear fraction, and reduced infection-induced translocation (Fig. 5*C*, Ad-Ctrl vs. Ad-Stx4, no cytokines; $P < 0.05$). These data indicate that the overexpression of Stx4 in human islet β-cells is associated with gene expression changes that may favor reduced apoptosis and the survival of more β-cells.

We next examined whether an Stx4-mediated reduction in cytokine-induced NF-κB translocation in islet β-cells could underlie the observed preserved β-cell mass in the STZ-challenged βTG-Stx4 mice. Indeed, we detected nuclear NF-κB and CC-3 staining in INS-1 832/13 cells transduced with Ad-RIP-Ctrl and then treated or not treated with proinflammatory cytokines (Fig. 6*A*, left

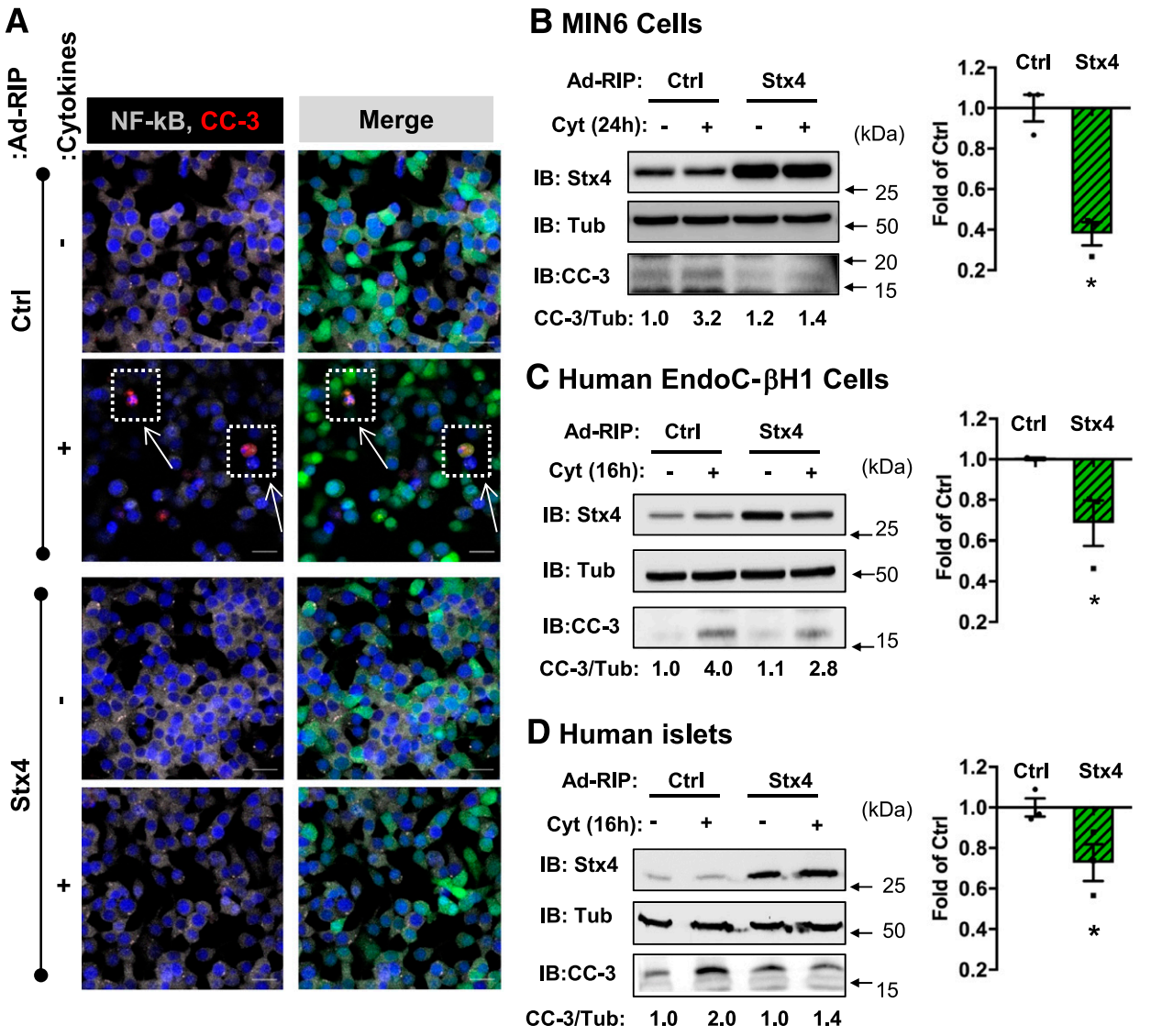

Figure 6—Cytokine (Cyt)-induced apoptosis is reduced in Stx4-overexpressing β-cells. *A*: INS-1 832/13 cells were transduced with Ad-RIP-Ctrl or Ad-RIP-Stx4 (green staining identifies adenovirus-transduced cells) and were subsequently exposed to a proinflammatory cytokine cocktail (TNF-α, IL-1β, IFN-γ) for 16 h before being fixed and immunostained for CC-3 and NF-κB. We used DAPI colocalization with NF-κB to evaluate NF-κB translocation to the nuclear compartment. Using blinded slides, among 300 cells we counted those that were GFP^+ for NF-κB (non)nuclear localization per treatment condition. We repeated this in three independent experiments using different cell passages (for a total of 900 cells per condition). Arrows denote the presence of cells showing CC-3 staining. Scale bar = 20 μm. *B*: MIN6 cells were transduced with Ad-RIP-Ctrl or Ad-RIP-Stx4 and subsequently exposed to the proinflammatory cytokine cocktail (TNF-α, IL-1β, IFN-γ) for 24 h. Apoptosis was assessed through the use of immunoblotting detergent cell lysate proteins for CC-3. Abundance of CC-3 in islets exposed to the cytokines (+Cyt) was normalized to tubulin (Tub), and the fold change over the control (−Cyt; Ctrl) was determined in three different passages of cells per treatment group (CC-3/Tub indicates the mean of results from three experiments for each treatment listed below the blots). *$P < 0.05$, Ad-RIP-Ctrl +Cyt vs. Ad-RIP-Stx4 +Cyt. *C*: Human EndoC-$βH^1$ β-cells were transduced and assessed as described for panel *B*. Data represent the mean of the results of three independent passages of cells per group. *$P < 0.05$, Ad-RIP-Ctrl +Cyt vs. Ad-RIP-Stx4 +Cyt. *D*: Human islets were transduced, exposed to proinflammatory cytokines for 16 h, and assessed as described for panel *B*. Data represent the mean of the results from three sets of donors islets per group. *$P < 0.05$, Ad-RIP-Ctrl +Cyt vs. Ad-RIP-Stx4 +Cyt. IB, immunoblot.

panels). Green fluorescent protein–positive (GFP^+) fluorescence was a marker of cells that were transduced with Ad-Ctrl or Ad-Stx4; we counted cells in a blinded manner (microscopists were blinded to the identities of the samples) and found that more than 86% of cells were GFP^+ in all groups. Of the 300 cells that were GFP^+ in each treatment group from each of three independent cell passages (a total of 900 cells per group), each was scored for nuclear CC-3-positive staining and for NF-κB (non)nuclear localization. In side-by-side comparisons, Ad-RIP-Ctrl cells showed two to three times more nuclear CC-3-positive cells (≥5% of the total, similar to prior findings [34]) than were seen among Ad-RIP-Stx4 cells (2% of the total). Moreover, only 10% of Ad-RIP-Stx4 cells showed nuclear NF-κB staining, whereas twice as many of the Ad-RIP-Ctrl cells did so (Fig. 6*A*, right panels). In a second approach, β-cells and human islets that were adenovirally transduced and exposed to proinflammatory cytokines were lysed and the CC-3 protein was detected and quantified by Western blotting. In MIN6 cells, Ad-RIP-Ctrl and cytokine exposure induced a 3.2-fold increase in CC-3 (Fig. 6*B*), and CC-3 expression was almost completed ablated in cells with Ad-RIP-Stx4 enrichment. The reduction in CC-3 expression positively correlated with the level of Stx4 overexpression in the human EndoC-βH^1 cell line and in primary human islets (Fig. 6*C* and *D*). This is, to our knowledge, the first demonstration of a *t*-SNARE protein such as Stx4 participating in an antiapoptotic manner.

DISCUSSION

We demonstrate, to our knowledge for the first time, that Stx4 enrichment correlates with decreased expression of chemokine ligand genes in human islets. Adenoviral transduction induced expression of chemokine ligands in the human islets: the control but not the Stx4-encoding adenovirus triggered chemokine gene expression. CXCL10 has been identified as a dominant chemokine ligand expressed in the islet environment of humans with T1D (33). Insulitic lesions of patients with T1D, but not pancreas donors without diabetes, showed CXCL10 expression, whereas islet-infiltrating leukocytes expressed the CXCL10 receptor, CXCR3 (35). Intervention in CXCL10/CXCR3 chemotaxis prevented autoimmune diabetes in mice (36,37). How does Stx4, a plasma membrane–localized exocytosis protein, affect the reprogramming of chemokine gene expression profiles? The originating expectation of the RNA sequencing studies was that vesicle-trafficking genes would be identified on the basis of the known role for Stx4 in exocytosis. Indeed, Stx3, also a plasma membrane–localized SNARE protein, is involved in trafficking immune mediators in dendritic cells (38). Stx3 and Stx4 have been implicated in antibody secretion by plasma cells (39). Stx4 has been loosely implicated in development, as it is required for exocytosis of GLUT8-containing vesicles with the plasma membrane to facilitate glucose uptake in mouse blastocysts for embryonic development (40), consistent with the role of Stx4 as a plasma membrane–localized *t*-SNARE protein. Stx4 decreased chemokine gene expression in human islet β-cells, concomitant with the ability to quench apoptosis (e.g., CC-3 display). Stx4 can be modified by *S*-nitrosylation in β-cells in response to cytokine stress (19), and hence it remains plausible that Stx4 overexpression provides additional unmodified Stx4 to functionally compensate (preserve normal GSIS) under stress conditions. However, how Stx4 overexpression quells stress-induced apoptosis and chemokine ligand gene expression is not evident from this perspective.

The three chemokine ligand genes—*CXCL9*, *CXCL10*, and *CXCL11*—are transactivated by NF-κB that has translocated to the nucleus (32,33,41). Exposure to metabolic, oxidative, or inflammatory stress in islets induces p38 and c-Jun N-terminal kinase mitogen-activated protein kinase signaling that promotes NF-κB to upregulate genes that promote apoptosis (42,43). Our data point to a decrease in NF-κB translocation to the nuclear fraction in human islets overexpressing Stx4 in their β-cells. Because Stx4 overexpression did not change the quantity of NF-κB, we assessed whether Stx4 was physically retaining NF-κB in the cytoplasmic compartment of human β-cells via a physical association; NF-κB was not found to coimmunoprecipitate with Stx4 in β-cells under any conditions tested. Hence, the detailed mechanism by which Stx4 overexpression suppresses NF-κB translocation remains to be determined.

It is interesting that RNA sequencing did not indicate changes in endoplasmic reticulum stress–related genes such as *ATF4* or *EIF2AK3*. Furthermore, β-cells transduced to overexpress Stx4 did not resist thapsigargin-induced endoplasmic reticulum stress (Supplementary Fig. 6). These studies add a new twist to the effects of stress on the death of β-cells in T1D (44,45). In addition to the production of the unfolded protein response and neoantigens that may provoke autoimmune responses against β-cells, we provide evidence for a defense mechanism of β-cells, through which Stx4 expression attenuates inflammatory stress–induced β-cell destruction, preserving functional β-cell mass. This effect may be selective to β-cells, because Stx4 has been implicated as a proapoptotic factor in a cancer cell line (46). Indeed, one could speculate that the combination of Stx4 acting to dampen β-cell stress while also killing cancer cells could provide an advantage in efforts to preserve functional β-cell mass.

In conclusion, Stx4 plays an unexpected role in controlling gene expression profiles that ultimately favors the preservation of islet β-cells. Human islet β-cells enriched for Stx4 correlated with a dampening of proinflammatory cytokine–induced apoptosis, coordinate with the retention of NF-κB in the cytosolic compartment and reduced expression of chemokine ligands affiliated with diabetes—namely, CXCL9, CXCL10, and CXCL11. Strikingly, the STZ-diabetes resistant phenotype of the βTG-Stx4 mice suggests that Stx4 upregulation is worthy of future

investigation in diabetes treatment and prevention, and in β-cell replacement strategies.

Acknowledgments. The authors are indebted to Heather N. Zook, Erika M. Olson, Arianne Aslamy, Karla E. Merz, and Mariann Chang (Diabetes and Metabolism Research Institute of City of Hope, Duarte, CA) for technical assistance with the subcellular fractionation, TUNEL, β-cell mass, and mouse studies, respectively. The authors thank Dr. Philipp Scherer (Diabetes and Metabolism Research Institute of City of Hope, Duarte, CA) for his generosity in providing the MIP-rtTA breeding stock.

Funding. This study was supported by grants from the National Institute of Diabetes and Digestive Kidney Diseases (grant nos. DK067912 and DK102233 to D.C.T.) and JDRF (grant no. 17-2013-454 to D.C.T.). The Southern California Islet Cell Resource Center (City of Hope) and the Integrated Islet Distribution Program (IIDP) supplied human islets. TRE-Stx4 transgenic mice were generated at the Indiana University School of Medicine Transgenic Mouse Core. Research reported in this publication also includes work performed at the City of Hope Islet Core, the Integrated Genomics Core (Charles Warden, bioinformatics), the Analytical Pharmacology Core, and the Light Microscopy Core, supported by the National Institutes of Health (award no. P30CA33572).

Duality of Interest. No potential conflicts of interest relevant to this article were reported.

Author Contributions. E.O. and M.A. researched data, contributed to the discussion, and reviewed and edited the manuscript. S.A. and T.C.B. provided the targeting vector reagents and protocols and edited the manuscript. B.O.R. contributed to the discussion and reviewed and edited the manuscript. D.C.T. conceived of the study; contributed to the discussion; and wrote, reviewed, and edited the manuscript. E.O., M.A., S.A., T.C.B., B.O.R., and D.C.T. read and approved the final version of the manuscript. D.C.T. is the guarantor of this work and, as such, had full access to all of the data in the study and takes responsibility for the integrity of the data and the accuracy of the data analysis.

References

1. Donath MY, Shoelson SE. Type 2 diabetes as an inflammatory disease. Nat Rev Immunol 2011;11:98–107
2. Eizirik DL, Colli ML, Ortis F. The role of inflammation in insulitis and beta-cell loss in type 1 diabetes. Nat Rev Endocrinol 2009;5:219–226
3. Bougneres PF, Carel JC, Castano L, et al. Factors associated with early remission of type I diabetes in children treated with cyclosporine. N Engl J Med 1988;318:663–670
4. Steffes MW, Sibley S, Jackson M, Thomas W. Beta-cell function and the development of diabetes-related complications in the diabetes control and complications trial. Diabetes Care 2003;26:832–836
5. Ferrannini E, Mari A, Nofrate V, Sosenko JM, Skyler JS; DPT-1 Study Group. Progression to diabetes in relatives of type 1 diabetic patients: mechanisms and mode of onset. Diabetes 2010;59:679–685
6. Gaisano HY. Recent new insights into the role of SNARE and associated proteins in insulin granule exocytosis. Diabetes Obes Metab 2017;19(Suppl. 1):115–123
7. Aslamy A, Thurmond DC. Exocytosis proteins as novel targets for diabetes prevention and/or remediation? Am J Physiol Regul Integr Comp Physiol 2017;312: R739–R752
8. Liang T, Qin T, Xie L, et al. New roles of syntaxin-1A in insulin granule exocytosis and replenishment. J Biol Chem 2017;292:2203–2216
9. Oh E, Stull ND, Mirmira RG, Thurmond DC. Syntaxin 4 up-regulation increases efficiency of insulin release in pancreatic islets from humans with and without type 2 diabetes mellitus. J Clin Endocrinol Metab 2014;99:E866–E870
10. Sadoul K, Lang J, Montecucco C, et al. SNAP-25 is expressed in islets of Langerhans and is involved in insulin release. J Cell Biol 1995;128:1019–1028
11. Spurlin BA, Park SY, Nevins AK, Kim JK, Thurmond DC. Syntaxin 4 transgenic mice exhibit enhanced insulin-mediated glucose uptake in skeletal muscle. Diabetes 2004;53:2223–2231
12. Spurlin BA, Thurmond DC. Syntaxin 4 facilitates biphasic glucose-stimulated insulin secretion from pancreatic beta-cells. Mol Endocrinol 2006;20: 183–193
13. Lam PP, Leung YM, Sheu L, et al. Transgenic mouse overexpressing syntaxin-1A as a diabetes model. Diabetes 2005;54:2744–2754
14. Berchtold LA, Størling ZM, Ortis F, et al. Huntingtin-interacting protein 14 is a type 1 diabetes candidate protein regulating insulin secretion and beta-cell apoptosis. Proc Natl Acad Sci U S A 2011;108:E681–E688
15. Yang C, Coker KJ, Kim JK, et al. Syntaxin 4 heterozygous knockout mice develop muscle insulin resistance. J Clin Invest 2001;107:1311–1318
16. Kusminski CM, Chen S, Ye R, et al. MitoNEET-parkin effects in pancreatic α- and β-Cells, cellular survival, and intrainsular cross talk. Diabetes 2016;65:1534–1555
17. Ye R, Wang M, Wang QA, et al. Autonomous interconversion between adult pancreatic α-cells and β-cells after differential metabolic challenges. Mol Metab 2016;5:437–448
18. Thurmond DC, Ceresa BP, Okada S, Elmendorf JS, Coker K, Pessin JE. Regulation of insulin-stimulated GLUT4 translocation by Munc18c in 3T3L1 adipocytes. J Biol Chem 1998;273:33876–33883
19. Wiseman DA, Kalwat MA, Thurmond DC. Stimulus-induced S-nitrosylation of syntaxin 4 impacts insulin granule exocytosis. J Biol Chem 2011;286:16344–16354
20. Ahn M, Yoder SM, Wang Z, et al. The p21-activated kinase (PAK1) is involved in diet-induced beta cell mass expansion and survival in mice and human islets. Diabetologia 2016;59:2145–2155
21. Chen YC, Colvin ES, Griffin KE, Maier BF, Fueger PT. Mig6 haploinsufficiency protects mice against streptozotocin-induced diabetes. Diabetologia 2014;57: 2066–2075
22. Oh E, Thurmond DC. Munc18c depletion selectively impairs the sustained phase of insulin release. Diabetes 2009;58:1165–1174
23. Oh E, Miller RA, Thurmond DC. Syntaxin 4 overexpression ameliorates effects of aging and high-fat diet on glucose control and extends lifespan. Cell Metab 2015;22:499–507
24. Becker TC, Noel RJ, Coats WS, et al. Use of recombinant adenovirus for metabolic engineering of mammalian cells. Methods Cell Biol 1994;43:161–189
25. Ravassard P, Hazhouz Y, Pechberty S, et al. A genetically engineered human pancreatic β cell line exhibiting glucose-inducible insulin secretion. J Clin Invest 2011;121:3589–3597
26. Oh E, Kalwat MA, Kim MJ, Verhage M, Thurmond DC. Munc18-1 regulates first-phase insulin release by promoting granule docking to multiple syntaxin isoforms. J Biol Chem 2012;287:25821–25833
27. Leiter EH. Multiple low-dose streptozotocin-induced hyperglycemia and insulitis in C57BL mice: influence of inbred background, sex, and thymus. Proc Natl Acad Sci U S A 1982;79:630–634
28. Zhang N, Schröppel B, Chen D, et al. Adenovirus transduction induces expression of multiple chemokines and chemokine receptors in murine beta cells and pancreatic islets. Am J Transplant 2003;3:1230–1241
29. Corbett JA, McDaniel ML. Does nitric oxide mediate autoimmune destruction of beta-cells? Possible therapeutic interventions in IDDM. Diabetes 1992;41: 897–903
30. Eizirik DL, Sammeth M, Bouckenooghe T, et al. The human pancreatic islet transcriptome: expression of candidate genes for type 1 diabetes and the impact of pro-inflammatory cytokines. PLoS Genet 2012;8:e1002552
31. Moore F, Naamane N, Colli ML, et al. STAT1 is a master regulator of pancreatic beta-cell apoptosis and islet inflammation. J Biol Chem 2011;286:929–941
32. Burke SJ, Goff MR, Lu D, Proud D, Karlstad MD, Collier JJ. Synergistic expression of the CXCL10 gene in response to IL-1β and IFN-γ involves NF-κB, phosphorylation of STAT1 at Tyr701, and acetylation of histones H3 and H4. J Immunol 2013;191:323–336
33. Sarkar SA, Lee CE, Victorino F, et al. Expression and regulation of chemokines in murine and human type 1 diabetes. Diabetes 2012;61:436–446

34. Hajmrle C, Ferdaoussi M, Plummer G, et al. SUMOylation protects against IL-1β-induced apoptosis in INS-1 832/13 cells and human islets. Am J Physiol Endocrinol Metab 2014;307:E664–E673
35. Roep BO, Kleijwegt FS, van Halteren AG, et al. Islet inflammation and CXCL10 in recent-onset type 1 diabetes. Clin Exp Immunol 2010;159:338–343
36. Homann D. Back from the brink: the uses of targeting the CXCL10:CXCR3 axis in type 1 diabetes. Diabetes 2015;64:3990–3992
37. Lasch S, Müller P, Bayer M, et al. Anti-CD3/Anti-CXCL10 antibody combination therapy induces a persistent remission of type 1 diabetes in two mouse models. Diabetes 2015;64:4198–4211
38. Collins LE, DeCourcey J, Rochfort KD, Kristek M, Loscher CE. A role for syntaxin 3 in the secretion of IL-6 from dendritic cells following activation of toll-like receptors. Front Immunol 2015;5:691
39. Gómez-Jaramillo L, Delgado-Pérez L, Reales E, et al. Syntaxin-4 is implicated in the secretion of antibodies by human plasma cells. J Leukoc Biol 2014;95:305–312
40. Wyman AH, Chi M, Riley J, et al. Syntaxin 4 expression affects glucose transporter 8 translocation and embryo survival. Mol Endocrinol 2003;17:2096–2102
41. Shin SY, Nam JS, Lim Y, Lee YH. TNFα-exposed bone marrow-derived mesenchymal stem cells promote locomotion of MDA-MB-231 breast cancer cells through transcriptional activation of CXCR3 ligand chemokines. J Biol Chem 2010; 285:30731–30740
42. Abdelli S, Ansite J, Roduit R, et al. Intracellular stress signaling pathways activated during human islet preparation and following acute cytokine exposure. Diabetes 2004;53:2815–2823
43. Ortis F, Pirot P, Naamane N, et al. Induction of nuclear factor-kappaB and its downstream genes by TNF-alpha and IL-1beta has a pro-apoptotic role in pancreatic beta cells. Diabetologia 2008;51:1213–1225
44. Brozzi F, Eizirik DL. ER stress and the decline and fall of pancreatic beta cells in type 1 diabetes. Ups J Med Sci 2016;121:133–139
45. Kracht MJ, van Lummel M, Nikolic T, et al. Autoimmunity against a defective ribosomal insulin gene product in type 1 diabetes. Nat Med 2017;23: 501–507
46. Perrotta C, Bizzozero L, Cazzato D, et al. Syntaxin 4 is required for acid sphingomyelinase activity and apoptotic function. J Biol Chem 2010;285:40240–40251